^{68}Ga-FAPI PET/CT: Tracer Uptake in 28 Different Kinds of Cancer

Clemens Kratochwil*[1], Paul Flechsig*[1,2], Thomas Lindner[1], Labidi Abderrahim[1], Annette Altmann[1,3], Walter Mier[1], Sebastian Adeberg[4,5], Hendrik Rathke[1], Manuel Röhrich[1], Hauke Winter[2,6], Peter K. Plinkert[7], Frederik Marme[8,9], Matthias Lang[10], Hans-Ulrich Kauczor[2,11], Dirk Jäger[12,13], Jürgen Debus[4,5,14], Uwe Haberkorn[1–3], and Frederik L. Giesel[1]

[1]Department of Nuclear Medicine, University Hospital Heidelberg, Heidelberg, Germany; [2]Translational Lung Research Center Heidelberg, German Center for Lung Research, Heidelberg, Germany; [3]Clinical Cooperation Unit Nuclear Medicine, German Cancer Research Center, Heidelberg, Germany; [4]Department of Radiation Oncology, University Hospital Heidelberg, Heidelberg, Germany; [5]Heidelberg Institute for Radiation Oncology, Heidelberg, Germany; [6]Department of Surgery, Thoraxklinik at University Hospital Heidelberg, Heidelberg, Germany; [7]Department of Otorhinolaryngology, Head and Neck Surgery, University Hospital Heidelberg, Heidelberg, Germany; [8]Department Obstetrics and Gynecology, University Hospital Heidelberg, Heidelberg, Germany; [9]Department Obstetrics and Gynecology, University Hospital Mannheim, Mannheim, Germany; [10]Department of Surgery, University Hospital Heidelberg, Heidelberg, Germany; [11]Department of Diagnostic and Interventional Radiology, University Hospital Heidelberg, Heidelberg, Germany; [12]Department of Medical Oncology and Internal Medicine VI, National Center for Tumor Diseases, University Hospital Heidelberg, Germany; [13]Clinical Cooperation Unit Applied Tumor Immunity, German Cancer Research Center, Heidelberg, Germany; and [14]Clinical Cooperation Unit Radiation Oncology, German Cancer Research Center, Heidelberg, Germany

The recent development of quinoline-based PET tracers that act as fibroblast-activation-protein inhibitors (FAPIs) demonstrated promising preclinical and clinical results. FAP is overexpressed by cancer-associated fibroblasts of several tumor entities. Here, we quantify the tumor uptake on ^{68}Ga-FAPI PET/CT of various primary and metastatic tumors to identify the most promising indications for future application. **Methods:** ^{68}Ga-FAPI PET/CT scans were requested by various referring physicians according to individual clinical indications that were considered insufficiently covered by ^{18}F-FDG PET/CT or other imaging modalities. All PET/CT was performed 1 h after injection of 122–312 MBq of ^{68}Ga-FAPI-04. We retrospectively identified 80 patients with histopathologically proven primary tumors or metastases or radiologically unequivocal metastatic lesions of histologically proven primary tumors. Tumor uptake was quantified by SUV_{max} and SUV_{mean} (60% isocontour). **Results:** Eighty patients with 28 different tumor entities (54 primary tumors and 229 metastases) were evaluated. The highest average SUV_{max} (>12) was found in sarcoma, esophageal, breast, cholangiocarcinoma, and lung cancer. The lowest ^{68}Ga-FAPI uptake (average SUV_{max} < 6) was observed in pheochromocytoma, renal cell, differentiated thyroid, adenoid cystic, and gastric cancer. The average SUV_{max} of hepatocellular, colorectal, head–neck, ovarian, pancreatic, and prostate cancer was intermediate (SUV 6–12). SUV varied across and within all tumor entities. Because of low background in muscle and blood pool (SUV_{max} < 2), the tumor-to-background contrast ratios were more than 3-fold in the intermediate and more than 6-fold in the high-intensity uptake group. **Conclusion:** Several highly prevalent cancers presented with remarkably high uptake and image contrast on ^{68}Ga-FAPI PET/CT. The high and rather selective tumor uptake may open up new applications for noninvasive tumor characterization, staging examinations, or radioligand therapy.

Key Words: FAPI; breast cancer; colorectal cancer; lung cancer; PET/CT

J Nucl Med 2019; 60:801–805
DOI: 10.2967/jnumed.119.227967

Several tumor entities, such as breast, colon, and pancreatic carcinomas, are characterized by a strong desmoplastic reaction (*1*). Cancer-associated fibroblasts and extracellular fibrosis can contribute up to 90% of the gross tumor mass, leaving original tumor cells in the minority (*2,3*). Many cancer-associated fibroblasts differ from normal fibroblasts by their relative specific expression of fibroblast activation protein (FAP). Therefore, FAP-specific inhibitors were first developed as anticancer drugs and then were consecutively advanced into tumor-targeting radiopharmaceuticals (*4,5*).

A biodistribution and initial dosimetry study of ^{68}Ga-FAP inhibitor (FAPI) PET/CT with 2 DOTA-containing ligands suggested that these tracers may expand and enrich the diagnostic cancer portfolio currently covered by ^{18}F-FDG (*6*). Moreover, the biodistribution suggested that ^{68}Ga-FAPI may be suitable for radioligand therapy (*7*). In view of the favorable initial results, ^{68}Ga-FAPI PET/CT was requested by various referring physicians on the basis of individual clinical indications. Often, scans were ordered to improve tumor delineation for planned surgery or radiotherapy. Thus, even lesions that were already unequivocally identified radiologically or by histopathology could be additionally characterized with ^{68}Ga-FAPI PET/CT.

The aim of this retrospective analysis was to quantify ^{68}Ga-FAPI uptake in a variety of primary, metastatic, or recurring cancers.

Received Mar. 5, 2019; revision accepted Mar. 19, 2019.
For correspondence or reprints contact: Clemens Kratochwil, Department of Nuclear Medicine, University Hospital Heidelberg, Im Neuenheimer Feld 400, 69120 Heidelberg, Germany.
E-mail: clemens.kratochwil@med.uni-heidelberg.de
*Contributed equally to this work.
Published online Apr. 6, 2019.

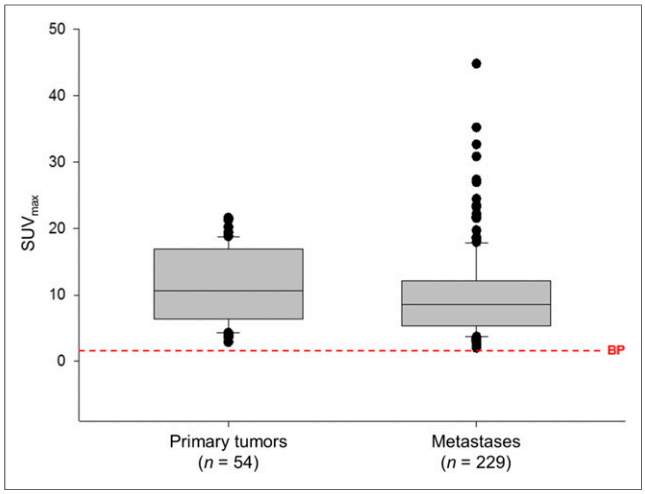

FIGURE 1. Neither mean, median, nor range of SUV_{max} of ^{68}Ga-FAPI-04 PET differs significantly between primary tumors and metastases.

MATERIALS AND METHODS

Patients

All patients were referred for experimental diagnostics by their treating oncologists, who were facing an unmet diagnostic challenge that could not be solved sufficiently with standard diagnostic means. Although the location and nature of tumor lesions were frequently known, the intent was to improve tumor delineation for reasons such as planning of radiotherapy. All patients gave written informed consent to receive ^{68}Ga-FAPI PET/CT on an individual-patient basis. The data were analyzed retrospectively with approval of the local ethics committee (approval S016/2018).

Radiopharmaceuticals

Synthesis and labeling of ^{68}Ga-FAPI-04 have already been described previously (*4*,*5*). Following the regulations of the German Pharmaceuticals Act §13(2b), the indication for the exam and labeling of the FAPI tracers was done under the direct responsibility of the applying physician. Injected activities were dependent on labeling yields. According to a previous dosimetry estimate—effective dose, 1.6 mSv/100 MBq (*6*)—an upper limit of 370 MBq regarding radiation exposure and a lower limit of 100 MBq per examination to achieve a sufficient count rate have been considered.

PET/CT Imaging

All imaging was performed on a Biograph mCT Flow scanner (Siemens). After non–contrast-enhanced low-dose CT (130 keV, 30 mAs, CareDose; reconstructed with a soft-tissue kernel to a slice thickness of 5 mm), PET was acquired in 3-dimensional mode (matrix, 200 × 200) using FlowMotion (Siemens). The emission data were corrected for randoms, scatter, and decay. Reconstruction was performed with an ordered-subset expectation maximization algorithm with 2 iterations/21 subsets and was Gauss-filtered to a transaxial resolution of 5 mm in full width at half maximum; attenuation correction was performed using the nonenhanced low-dose CT data. The injected activity for the ^{68}Ga-FAPI examinations was 122–312 MBq, and the PET scans were started 1 h after injection. A 500-mL volume of saline with 20 mg of furosemide was infused from 15 min before to 30 min after tracer application. The patients were asked to self-report any abnormalities 30 min after finishing the examination.

Imaging Evaluation

Tumor tracer uptake was quantified by SUV_{mean} and SUV_{max} at 1 h after injection. For calculation of the SUV, circular regions of interest were drawn around the tumor lesions with focally increased uptake in transaxial slices and automatically adapted to a 3-dimensional volume of interest with e.soft software (Siemens) at a 60% isocontour. The unspecific background in blood pool (aortic vessel content) and muscle was quantified with a circular 2-cm-diameter sphere.

RESULTS

Adverse Events

All patients tolerated the examination well. No drug-related pharmacologic effects or physiologic responses occurred. During injection and the 1.5 h of follow-up, no patient reported any new symptoms.

Quantifying ^{68}Ga-FAPI Uptake in Primary Tumors and Metastatic Disease

Patient numbers were not sufficient to compare the SUVs of primary tumors versus metastases for individual cancers. The overall SUV mean (11.5 ± 5.5 vs. 10.0 ± 6.3), median (10.7 vs. 8.5), and range (2.9–21.6 vs. 2.0–44.8) of ^{68}Ga-FAPI in primary tumors (n = 54) and metastatic lesions (n = 229) did not differ (Fig. 1). Subsequently, we analyzed primary and metastatic lesions of individual tumor entities in a pooled fashion.

The highest average SUV_{max} (>12) was found in sarcoma, esophageal, breast, cholangiocarcinoma, and lung cancer. The lowest ^{68}Ga-FAPI uptake (average SUV_{max} < 6) was observed in renal cell, differentiated thyroid, adenoid cystic, gastric, and pheochromocytoma cancer. The average SUV_{max} of hepatocellular, colorectal, head–neck, ovarian, pancreatic, and prostate cancer was

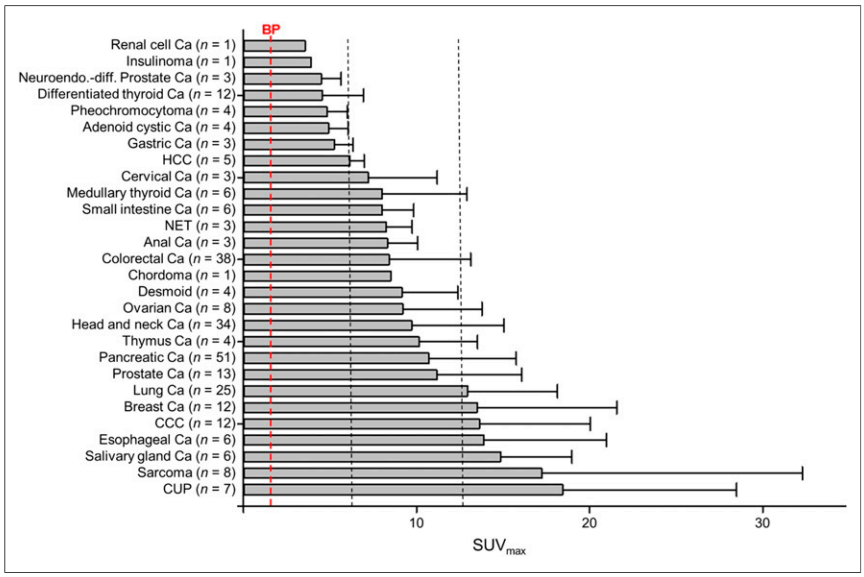

FIGURE 2. Average SUV_{max} of ^{68}Ga-FAPI PET/CT in various tumor entities. Low, intermediate, and high uptake was defined by cutoff at SUVs 6 and 12. By comparison, average background (blood pool) was found to have SUV 1.4. Ca = cancer; CCC = cholangiocellular carcinoma; CUP = carcinoma of unknown primary; HCC = hepatocellular carcinoma; NET = neuroendocrine tumor.

intermediate (SUV 6–12). All tumor entities exhibited a high interindividual SUV variation (Fig. 2). Because of the low background activity (average SUV_{mean} of blood pool and muscle, 1.2 and 1.0, respectively; SUV_{max}, 1.6 and 1.4, respectively), the tumor-to-background ratios are more than 3 in the intermediate and more than 6 in the high-intensity uptake group (Fig. 2). These high ratios resulted in high image contrast and excellent tumor delineation in most of the evaluated patients (Fig. 3).

DISCUSSION

The aim of this retrospective analysis was to quantify the uptake of ^{68}Ga-FAPI ligand in different types of cancer.

The highest uptake (average $SUV_{max} > 12$) was found in lung, breast, and esophageal cancer; cholangiocellular carcinoma; and sarcoma. This may open indications for ^{68}Ga-FAPI PET/CT for cases in which ^{18}F-FDG PET/CT faces its limitations. Because of low uptake of ^{18}F-FDG in low-grade sarcomas, there is a wide overlap between benign and malignant lesions, and even dual–time-point imaging could not eliminate this well-known limitation of ^{18}F-FDG PET/CT (*8,9*). The main limitation of ^{18}F-FDG PET/CT in staging of esophageal cancer is its low to moderate sensitivity for lymph node staging (*10*) and delineation between viable tumor and regional esophagitis. In breast cancer, ^{18}F-FDG PET/CT is commonly used in recurrence but not generally recommended for initial staging (*11*). Cholangiocarcinoma exhibits considerable variability in ^{18}F-FDG uptake, which was correlated with a weak expression of hexokinase-2 (*12*). ^{18}F-FDG PET/CT performs well in lung cancer; however, high cerebral background requires brain MRI for complete staging (*13*). Thus, these tumors may benefit from ^{68}Ga-FAPI PET/CT imaging. However, the limited number of patients examined by ^{68}Ga-FAPI PET/CT until now does not allow subgroup analysis of histologic variants or differentiation grades.

Surprisingly, colon and pancreatic cancers, that is, the ones with the highest desmoplastic reaction by histopathology (*3*), demonstrated only intermediate ^{68}Ga-FAPI uptake (SUV 6–12). The liver is the first target organ for metastases of colorectal cancer. We already reported a significantly lower hepatic background for ^{68}Ga-FAPI (SUV 1.7) than for ^{18}F-FDG (SUV 2.8). This may be advantageous for liver metastasis detection (*6*). Within the patients reported here, we identified liver metastases as small as 1 cm in diameter (Fig. 4). Because of its limited sensitivity of 30% for detecting lymph node metastasis (*14*) and false-positive findings in acute pancreatitis, ^{18}F-FDG PET is of limited usefulness for surgical planning in pancreatic cancer (*15*). Thus, even intermediate uptake in ^{68}Ga-FAPI PET/CT presents a reasonable perspective to improve clinical diagnostic performance. In ovarian cancer, another tumor in the intermediate-intensity group, ^{18}F-FDG can overcome some limits of conventional imaging but, because of peristaltic activity, often suffers from heterogeneous uptake in the intestinal wall (*16,17*). In contrast, ^{68}Ga-FAPI demonstrates very low unspecific intestinal/peritoneal uptake and might be superior to identify peritoneal carcinomatosis, the main clinical challenge of advanced-stage ovarian cancer. Head–neck tumors often go along with local inflammation. Unfortunately, a recent review reported that most original work found that ^{18}F-FDG PET/CT is not useful in discriminating benign from malignant tumors because of the overlap of uptake in both conditions (*18–20*). In this setting, ^{68}Ga-FAPI PET/CT may offer an advantage regarding tumor delineation—for example, in planning of radiotherapy (Fig. 5). Differentiation between residual/recurrent disease and postchemoradiation fibrosis was reported to be a diagnostic challenge for ^{18}F-FDG (*21*). It should be mentioned that unspecific fibrosis may also cause issues for ^{68}Ga-FAPI PET; however, because of the inherent difference in normal activated fibroblasts and cancer-associated fibroblasts (*4,5*), this possibility

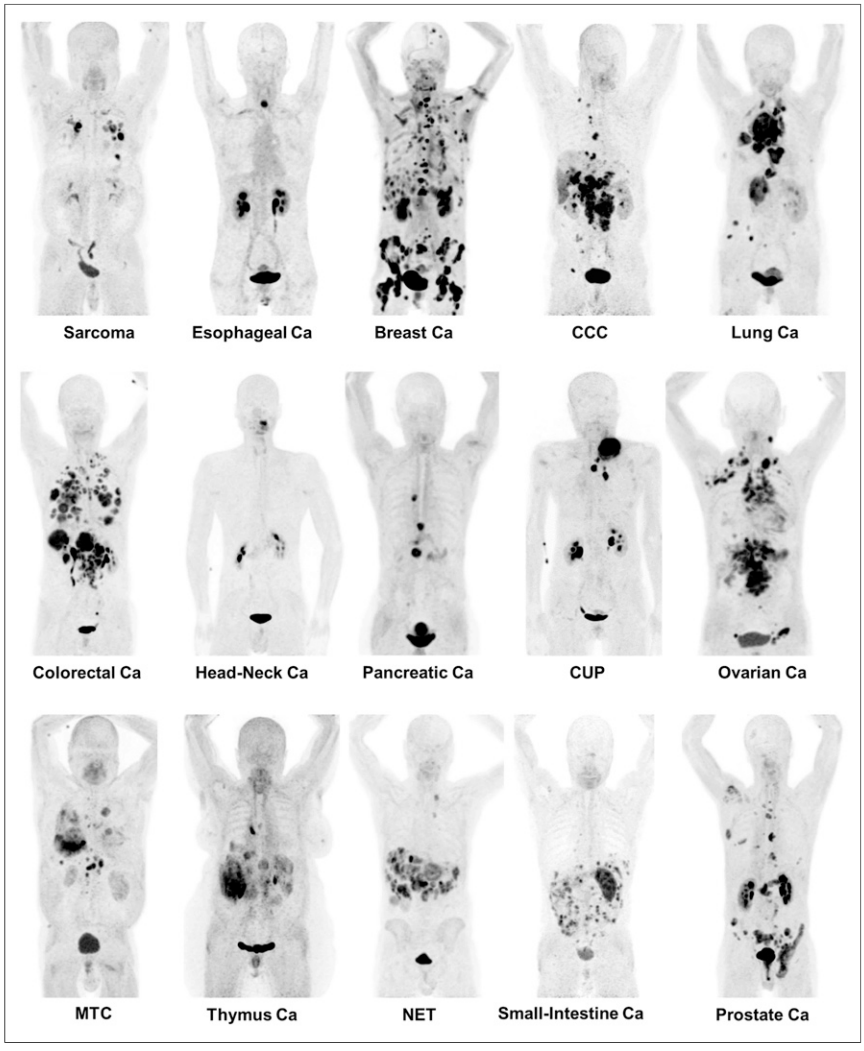

FIGURE 3. Maximum-intensity projections of ^{68}Ga-FAPI PET/CT in patients reflecting 15 different histologically proven tumor entities (sorted by uptake in descending order). Ca = cancer; CCC = cholangiocellular carcinoma; CUP = carcinoma of unknown primary; MTC = medullary thyroid cancer; NET = neuroendocrine tumor.

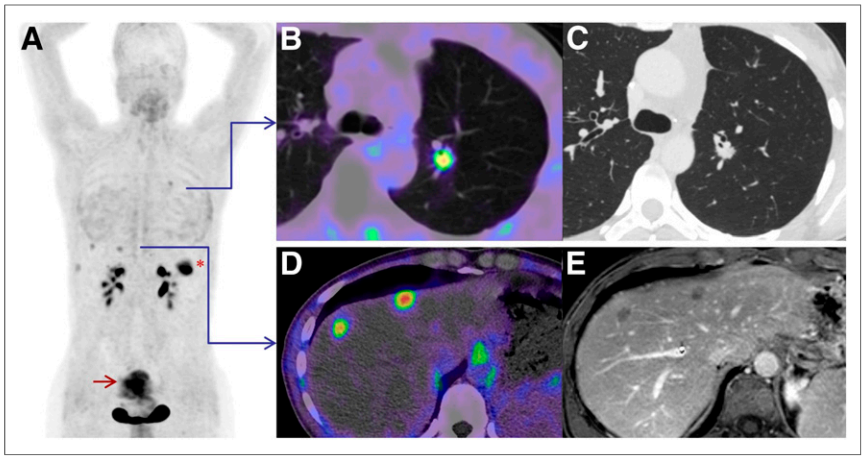

FIGURE 4. Maximum-intensity projection (A) of patient with colorectal carcinoma. Because of low physiologic background uptake, tiny lesions in lung (B) and liver (D) were detected by ^{68}Ga-FAPI-04 PET/CT and measured in dedicated CT of lung (C) and hepatic MRI (E) with long-axis diameters of 1 cm. *Primary tumor in left colon flexure. Red arrow = unspecific uptake in uterus.

still needs to be proven. Intermediate to high ^{68}Ga-FAPI uptake was also observed in prostate cancer. However, only patients with prostate-specific membrane antigen–negative tumors, which are the minority of prostate cancers, were selected to receive additional ^{68}Ga-FAPI PET/CT, and because of this selection bias, our cohort does not reflect typical patients.

^{18}F-FDG PET often performs poorly in renal cell carcinoma, pheochromocytoma, and neuroendocrine tumors, including medullary thyroid cancer and insulinomas. This limitation is unlikely to be overcome, because SUVs for these tumors are also low for ^{68}Ga-FAPI (average $SUV_{max} < 6$). This is likely not a significant problem because several special PET tracers such as ^{18}F-DOPA for neuroblastoma/pheochromocytoma (*22*), ^{68}Ga-labeled somatostatin analogs for neuroendocrine tumors (*23*), ^{89}Zr-girentuximab for renal cell carcinoma (*24*), and ^{68}Ga-exendin targeting glucagon-like peptide-1 receptor on insulinoma (*25*) recently closed this gap.

The current imaging findings are largely consistent with histopathology reports. FAP expression on activated fibroblasts in tumor stroma was already quantified in 1990 using the antibody-F19 (*3*). Well in line with our results, a weak desmoblastic reaction was observed in renal cell cancer and neuroblastoma/pheochromocytoma; intermediate staining in pancreatic, gastric, endometrial/cervix cancer; and high expression in breast cancer (*3*). In contrast to this historical paper, we found a higher ^{68}Ga-FAPI uptake in neuroendocrine tumors (intermediate group in ^{68}Ga-FAPI PET, weak in histology) and lung cancer (high uptake in ^{68}Ga-FAPI PET, intermediate in histology). For colorectal cancer, which was the most commonly high-expressing tumor in the work of Garin-Chesa et al. (*3*), we only measured intermediate values. Low case numbers, heterogeneity of expression, random effects in tissue sampling, and high interindividual variability appear the most appropriate explanations for these differences between histologic in vitro and imaging in vivo results. Another explanation and also a possible reason for the high interindividual variability can be patient selection. Immunohistochemical work-up has primarily been performed in early-stage nonmetastatic, and thus rather indolent, tumors. In contrast, the patients evaluated by ^{68}Ga-FAPI PET/CT are a more heterogeneous group. Most presented with recurrent and metastatic disease and sometimes (most frequently in colorectal cancer patients) even after several lines of systemic therapy. We also want to emphasize that the aim of this work was only to characterize true-positive lesions (proven by histopathology or unequivocal radiologic findings of histopathologically proven primary tumors), as no acceptable gold standard to rule out false-negative findings was available. Thus, sensitivity and overall diagnostic accuracy cannot be determined.

FAP was considered a promising target for nuclear-labeled tumor probes in 1994. Because of tumor-to-liver ratios of up to 21:1, the antibody ^{131}I-mAb-F19 could delineate liver metastases of colorectal cancer as small as 1 cm in diameter (*26*). This was confirmed by our observations (Fig. 4) and is supported by earlier data that cancer-associated fibroblasts are already found in lesions above 1–2 mm in diameter (*27*). However, well in line with typical antibody kinetics, the optimal time for tumor imaging with ^{131}I-mAb-F19 was 3–5 d after administration (*26*). In contrast, ^{68}Ga-FAPI PET/CT can be performed 10 min to 1 h after administration and, in contrast to ^{18}F-FDG studies, can be done without fasting and resting time (*6*). This is a potential operational advantage, as observed between prostate-specific membrane antigen targeting with the antibody J591 and an optimal imaging after 6–8 d (*28*) versus low-molecular-weight prostate-specific membrane antigen ligands that can be imaged 1 h after injection (*29*).

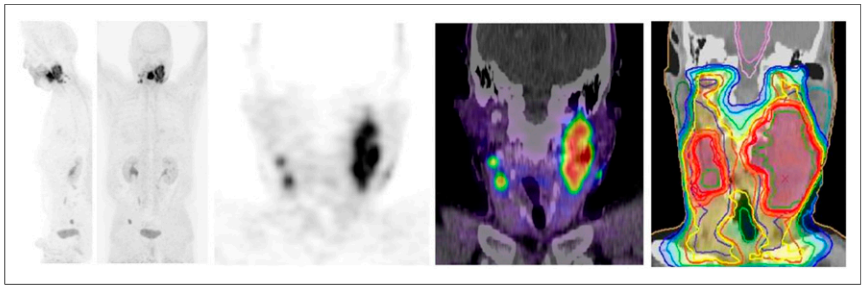

FIGURE 5. Among others, one clinical application for ^{68}Ga-FAPI PET/CT can be to improve gross tumor volume delineation in preparation for external-beam radiotherapy—in this case, squamous cell carcinoma of neck with local lymph node metastases. From left to right: whole-body maximum-intensity projections, coronal PET slice through head/neck tumor, its fusion with coregistered CT, PET-segmented target-volume definition for external-beam radiotherapy.

CONCLUSION

Several epidemiologically important tumor entities, in particular breast, esophagus, lung, pancreatic, head–neck, and colorectal cancer, present with a remarkably high uptake in ^{68}Ga-FAPI PET/CT. This may open new applications for noninvasive tumor characterization and staging examinations. Because the ^{68}Ga-FAPI tracers contain the universal DOTA chelator, also a theranostic approach—after labeling the ligand with an appropriate therapeutic radionuclide—seems feasible. Other known ^{18}F-FDG limitations, for example, in differentiated thyroid

and renal cell carcinoma, can probably not be overcome with ^{68}Ga-FAPI. The limitations of this report, such as retrospective evaluation, a heterogeneous patient collective, and a low case number for some kinds of tumor, require further studies.

DISCLOSURE

A patent application for quinoline-based FAP-targeting agents for imaging and therapy in nuclear medicine presents a potential financial conflict of interest for authors Clemens Kratochwil, Thomas Lindner, Walter Mier, Uwe Haberkorn, and Frederik Giesel. No other potential conflict of interest relevant to this article was reported.

REFERENCES

1. Siveke JT. Fibroblast-activating protein: targeting the roots of the tumor microenvironment. *J Nucl Med.* 2018;59:1412–1414.
2. Hamson EJ, Keane FM, Tholen S, Schilling O, Gorrell MD. Understanding fibroblast activation protein (FAP): substrates, activities, expression and targeting for cancer therapy. *Proteomics Clin Appl.* 2014;8:454–463.
3. Garin-Chesa P, Old LJ, Rettig WJ. Cell surface glycoprotein of reactive stromal fibroblasts as a potential antibody target in human epithelial cancers. *Proc Natl Acad Sci USA.* 1990;87:7235–7239.
4. Loktev A, Lindner T, Mier W, et al. A tumor-imaging method targeting cancer-associated fibroblasts. *J Nucl Med.* 2018;59:1423–1429.
5. Lindner T, Loktev A, Altmann A, et al. Development of quinoline based theranostic ligands for the targeting of fibroblast activation protein. *J Nucl Med.* April 6, 2018 [Epub ahead of print].
6. Giesel F, Kratochwil C, Lindner T, et al. ^{68}Ga-FAPI PET/CT: biodistribution and preliminary dosimetry estimate of 2 DOTA-containing FAP-targeting agents in patients with various cancers. *J Nucl Med.* 2019;60:386–392.
7. Loktev A, Lindner T, Burger EM, et al. Development of novel FAP-targeted radiotracers with improved tumor retention. *J Nucl Med.* March 8, 2019 [Epub ahead of print].
8. Parghane RV, Basu S. Dual-time point ^{18}F-FDG-PET and PET/CT for differentiating benign from malignant musculoskeletal lesions: opportunities and limitations. *Semin Nucl Med.* 2017;47:373–391.
9. Tagliabue L, Del Sole A. Appropriate use of positron emission tomography with [^{18}F]fluorodeoxyglucose for staging of oncology patients. *Eur J Intern Med.* 2014; 25:6–11.
10. Jiang C, Chen Y, Zhu Y, Xu Y. Systematic review and meta-analysis of the accuracy of ^{18}F-FDG PET/CT for detection of regional lymph node metastasis in esophageal squamous cell carcinoma. *J Thorac Dis.* 2018;10:6066–6076.
11. Caresia Aroztegui AP, García Vicente AM, Alvarez Ruiz S, et al. ^{18}F-FDG PET/CT in breast cancer: evidence-based recommendations in initial staging. *Tumour Biol.* 2017;39:1010428317728285.
12. Paudyal B, Oriuchi N, Paudyal P, et al. Clinicopathological presentation of varying ^{18}F-FDG uptake and expression of glucose transporter 1 and hexokinase II in cases of hepatocellular carcinoma and cholangiocellular carcinoma. *Ann Nucl Med.* 2008;22:83–86.
13. Flechsig P, Mehndiratta A, Haberkorn U, Kratochwil C, Giesel FL. PET/MRI and PET/CT in lung lesions and thoracic malignancies. *Semin Nucl Med.* 2015; 45:268–281.
14. Kauhanen SP, Komar G, Seppänen MP, et al. A prospective diagnostic accuracy study of ^{18}F-fluorodeoxyglucose positron emission tomography/computed tomography, multidetector row computed tomography, and magnetic resonance imaging in primary diagnosis and staging of pancreatic cancer. *Ann Surg.* 2009; 250:957–963.
15. Strobel O, Büchler MW. Pancreatic cancer: FDG-PET is not useful in early pancreatic cancer diagnosis. *Nat Rev Gastroenterol Hepatol.* 2013;10:203–205.
16. Marzola MC, Chondrogiannis S, Rubello D. Fludeoxyglucose F 18 PET/CT assessment of ovarian cancer. *PET Clin.* 2018;13:179–202.
17. Kitajima K, Murakami K, Sakamoto S, Kaji Y, Sugimura K. Present and future of FDG-PET/CT in ovarian cancer. *Ann Nucl Med.* 2011;25:155–164.
18. Bertagna F, Nicolai P, Maroldi R, et al. Diagnostic role of ^{18}F-FDG-PET or PET/CT in salivary gland tumors: a systematic review. *Rev Esp Med Nucl Imagen Mol.* 2015;34:295–302.
19. Zafereo ME. Evaluation and staging of squamous cell carcinoma of the oral cavity and oropharynx: limitations despite technological breakthroughs. *Otolaryngol Clin North Am.* 2013;46:599–613.
20. Plaxton NA, Brandon DC, Corey AS, et al. Characteristics and limitations of FDG PET/CT for imaging of squamous cell carcinoma of the head and neck: a comprehensive review of anatomy, metastatic pathways, and image findings. *AJR.* 2015;205:W519–W531.
21. Lai V, Khong PL. Updates on MR imaging and ^{18}F-FDG PET/CT imaging in nasopharyngeal carcinoma. *Oral Oncol.* 2014;50:539–548.
22. Amodru V, Guerin C, Delcourt S, et al. Quantitative ^{18}F-DOPA PET/CT in pheochromocytoma: the relationship between tumor secretion and its biochemical phenotype. *Eur J Nucl Med Mol Imaging.* 2018;45:278–282.
23. Barrio M, Czernin J, Fanti S, et al. The impact of somatostatin receptor-directed PET/CT on the management of patients with neuroendocrine tumor: a systematic review and meta-analysis. *J Nucl Med.* 2017;58:756–761.
24. Hekman MCH, Rijpkema M, Aarntzen EH, et al. Positron emission tomography/computed tomography with ^{89}Zr-girentuximab can aid in diagnostic dilemmas of clear cell renal cell carcinoma suspicion. *Eur Urol.* 2018;74:257–260.
25. Antwi K, Fani M, Heye T, et al. Comparison of glucagon-like peptide-1 receptor (GLP-1R) PET/CT, SPECT/CT and 3T MRI for the localisation of occult insulinomas: evaluation of diagnostic accuracy in a prospective crossover imaging study. *Eur J Nucl Med Mol Imaging.* 2018;45:2318–2327.
26. Welt S, Divgi CR, Scott AM, et al. Antibody targeting in metastatic colon cancer: a phase I study of monoclonal antibody F19 against a cell-surface protein of reactive tumor stromal fibroblasts. *J Clin Oncol.* 1994;12:1193–1203.
27. Davidson B, Goldberg I, Kopolovic J. Inflammatory response in cervical intraepithelial neoplasia and squamous cell carcinoma of the uterine cervix. *Pathol Res Pract.* 1997;193:491–495.
28. Pandit-Taskar N, O'Donoghue JA, Beylergil V, et al. ^{89}Zr-huJ591 immuno-PET imaging in patients with advanced metastatic prostate cancer. *Eur J Nucl Med Mol Imaging.* 2014;41:2093–2105.
29. Afshar-Oromieh A, Hetzheim H, Kübler W, et al. Radiation dosimetry of ^{68}Ga-PSMA-11 (HBED-CC) and preliminary evaluation of optimal imaging timing. *Eur J Nucl Med Mol Imaging.* 2016;43:1611–1620.